Theoretical Analysis of Ultrafast Fluorescence Depletion of Vibrational Relaxation of Dye Molecules in Solution

Yong He, Yijia Xiong, Zhaohui Wang, Qihe Zhu, and Fanao Kong*

Institute of Chemistry, The Chinese Academy of Sciences, Beijing 100080, China

Received: October 7, 1997; In Final Form: December 18, 1997

Ultrafast vibrational relaxation and solvation dynamics of electronically excited dye molecules in solution are theoretically studied on the basis of the perturbative density operator method and the transient linear susceptibility theory. Femtosecond time-resolved profile of the stimulated emission pumping fluorescence depletion (SEP FD) is simulated with a single vibrational mode. The results show that the fast and the slow SEP components reflect primarily the vibrational relaxation and the solvation effect, respectively, in the first excited state S_1 of the dye molecules.

I. Introduction

Following an optical excitation of a solute molecule in polar solvent, two ultrafast dynamic processes will take place. One is the vibrational relaxation in the electronic excited state. The other process is known as excited-state solvation. The studies have been reviewed by some authors.[1−6] It is important to understand the vibrational relaxation pathways and rates, especially whether the route is through intramolecular vibrational redistribution (IVR) to other modes or through external vibrational relaxation (EVR) to the solvent.

As to the theory of vibrational relaxation in liquids, many important advances have been made by a large number of workers.[7−12] Owing to the connection between solvation dynamics and the solvent's dielectric response, a number of more advanced theories have been developed,[13−15] and computer simulations have played an important role in our understanding of the mechanism of solvation.[16−20] In the theoretical description of the time-dependent response of the material system, the ultrafast dynamics enters through the laser-induced nonlinear polarization, which has to be evaluated for the appropriate model system. Most of the theoretical work has employed a perturbative description for the interaction of the molecular system with the laser field.[21−25] More recently, nonperturbative descriptions have been considered[26−30] also.

The advent of picosecond and femtosecond laser spectroscopy has made possible the study of vibrational relaxation and the excited-state solvation of polyatomic molecules. The ultrafast vibronic responses of dyes IR125,[31] sulforhodamine B,[32] cresyl violet, and rhodamine[33,34] have been studied in pump−probe experiments. Time-resolved fluorescence measurements have yielded information concerning vibrational relaxation of nile blue,[35] oxazine-1, and malachite green.[36] A popular method of studying solvation dynamics is to measure the shift of the spectrum of the solute molecules. Time-resolved emission measurements of coumarin 153,[37] LDS750,[38,39] and styryl dye DASPI[40] were used to probe the time dependence of solvation. Recently, in our group a femtosecond time-resolved stimulated emission pumping fluorescence depletion (FS TR SEP FD) method[41] has been developed to study the vibrational relaxation of the electronic excited state of dye molecules in solution.

* Author for correspondence. Email address: kong@mrdlab.icas.ac.cn.

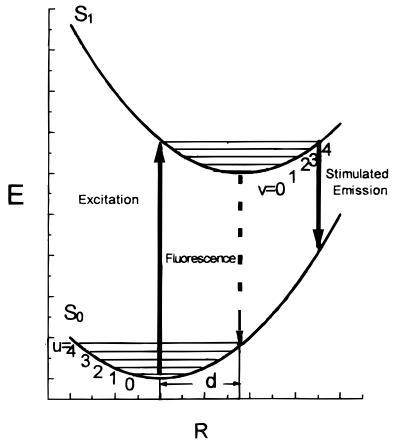

Figure 1. Schematic diagram of the electronic transitions and fluorescence emission.

To get some physical interpretation of our observed spectra,[41] we perform some theoretical calculations on FS TR SEP FD of dye LDS698, LDS751, and LDS765 and determine preliminarily the vibrational transition rate and two parameters relating to the solvation of these dye molecules. Using these theories, Lin et al. have analyzed the femtosecond time-resolved spectra of *Rhodobacter sphaeroides* in their previous work.[42] Here, we apply also similar methods in the present work.

II. Steady-State and Femtosecond Time-Resolved Spectra

The principle of the time-resolved stimulated emission pumping fluorescence depletion method[41] (TR SEP FD) is the following. A femtosecond laser pulse is used to excite the molecules from the ground-state S_0 to an excited-state S_1. After a delay time τ, a second femtosecond laser pulse is applied to the excited molecules to induce stimulated emission with a transition from the excited vibronic manifold $\{v\}$ to the ground vibronic manifold $\{u\}$ (Figure 1).

Three dyes, LDS698, LDS751, and LDS765, dissolved in PC:EG (a mixture of $C_4H_6O_3$ and ethylene glycol $CH_3CHOHCH_2$-OH, volume ratio of 1:4) have been investigated.[41] From the conventional absorption and fluorescence spectra (Figure 2), we estimate that the 0−0 transitions of LDS698, LDS751, and LDS765 are at 556 nm (18 000 cm^{-1}), 625 nm (16 000cm^{-1}), and 690 nm (14 500 cm^{-1}), respectively.

S1089-5639(97)03256-8 CCC: $15.00
Published on Web 04/04/1998

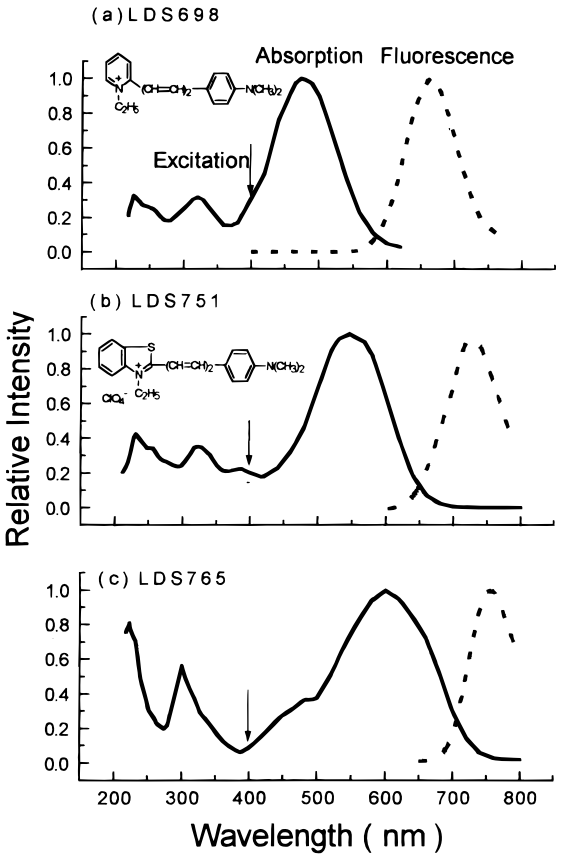

Figure 2. Steady-state absorption and fluorescence spectra of LDS698 (a), LDS751 (b), and LDS765 (c).

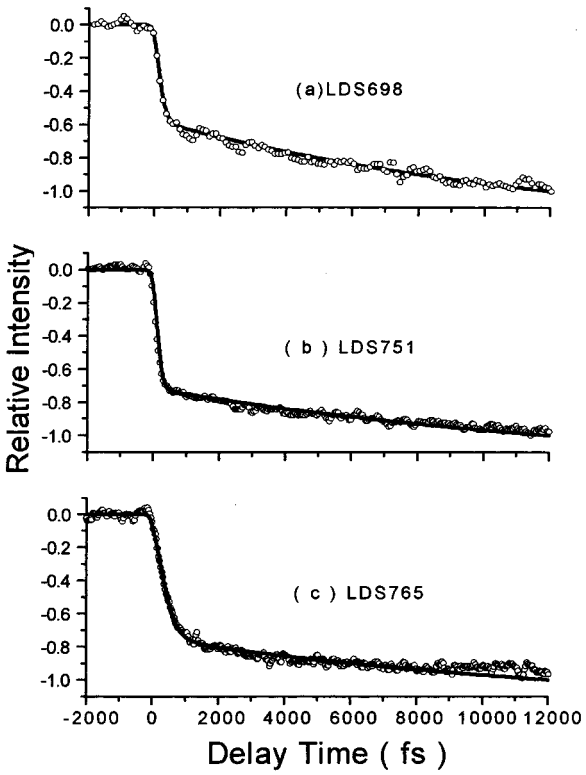

Figure 3. Time-resolved stimulated emission pumping fluorescence depletion of the LDS698, LDS751, and LDS765 dye solutions. The open circles represent experimental data, and the lines represent simulated results.

Since the wavelength of the excitation laser was 398 nm (25 126 cm^{-1}), the excess vibrational energies are 7000, 9000, and 10 500 cm^{-1} for the three dye molecules, respectively. Although there are many vibrational modes for each molecule, only a few Franck−Condon transition active modes contribute to the vibronic S_0-S_1 transitions. Each dye molecule we studied contains at least two phenyl or heteraromatic rings. The quadrant stretching and the semicircle stretching of the ring vibration cause a fairly strong absorption in the 1600 and 1500 cm^{-1} regions, respectively.[43] The analogous vibrations were also investigated by other authors. Kaiser et al.[44] in their ultrafast study of oxazine-1 took 1400 cm^{-1} as the active mode in their simulation. Elsaesser et al.[32] investigated the ultrafast relaxation of the 1350 cm^{-1} skeletal mode of sulforhodamine B. In this paper, we also assume that the Franck−Condon active mode is the ring skeletal vibration with a frequency of 1500 cm^{-1}. The relational excitation reached vibrational levels of $v = 4$, 5, and 6 of the S_1 state for LDS698, LDS751, and LDS765, respectively.

Because of the anharmonic coupling among different intramolecular vibration modes and the instantaneous normal modes of the liquid bath, the vibrational excitation in S_1 state is quickly relaxed to the lowest level with a time constant of 1 ps. At the $v = 0$ state, a slower process of the excited-state solute−solvent interaction with a time scale of 1−10 ps takes place. Meanwhile, much slower spontaneous emission fluorescence with a lifetime of a few hundred picoseconds also happens. The fluorescence signal is recorded and shown in Figure 3. On the left, the flat plateau indicates the 398 nm excitation laser-induced fluorescence. The intense SEP laser pulse depopulates the S_1 state, causing a depletion of the fluorescence, also shown in Figure 3. A further analysis of the SEP signal reveals that the fast and the slow decay components reflect the vibrational relaxation and the excited-state solvation of the molecule, respectively.

III. Theoretical Model

After the dye molecule at vibrational level $u = 0$ of the S_0 state is excited to a specific vibrational level v_m of the S_1 state, the SEP laser pulse stimulates the transition of the molecule from the upper vibronic manifold $\{v\}$ to the lower vibronic manifold $\{u\}$. On the basis of the perturbative density operator method and the transient linear susceptibility theory,[24,42,45−48] the time-resolved incoherent part of the intensity of the stimulated emission can be given by

$$I(\omega_{pr}, \tau) = C_0 \sum_{v=0}^{v_m} \rho_{v,v}(\tau) B_{v,v}(\omega_{pr}, \tau) \quad (1)$$

where C_0 is a coefficient, ω_{pr} is the central frequency of the SEP pulse, and the element of density matrax $\rho_{v,v}$ denotes the vibrational population of the S_1 state. The sum is over all vibrational levels from 0 to v_m.

$B_{v,v}$ is a SEP coefficient relating to stimulated emission effect. In the Condon approximation, the SEP coefficient can be written as

$$B_{v,v}(\omega_{pr}, \tau) = \frac{-(\vec{\mu}_{s1,s0} \otimes \vec{\mu}_{s0,s1})}{\hbar} F_{v,v}(\omega_{pr})\{1 + C_1[1 - \exp(-k\tau)]\} \quad (2)$$

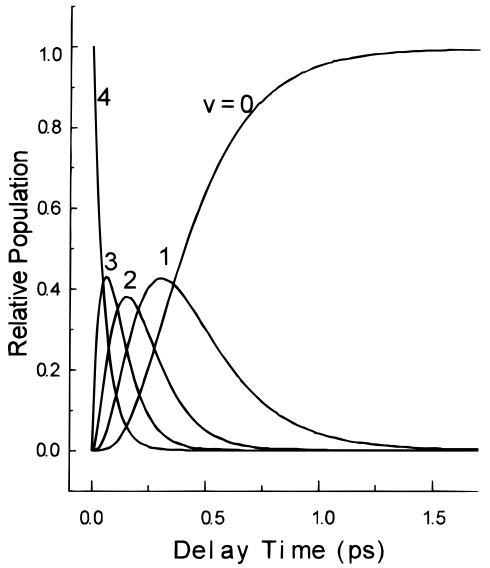

Figure 4. Temporal evolution of the relative population of various vibrational levels for dye LDS698.

where μ represents the transition dipole moment. The band-shape function is given as

$$F_{v,v}(\omega_{pr}) = \sum_{u=0}^{u_m} |\langle s_0 u | s_1 v \rangle|^2 \frac{2/\Gamma_{pr}}{(\omega_{s1v,s0u} - \omega_{pr})^2 + (2/\Gamma_{pr})^2} \quad (3)$$

where $\omega_{s1v,s0u} = \omega_{s1,s0} + (v - u)\omega$. $\omega_{s1,s0}$ is the 0−0 band transition frequency, and ω is the vibrational frequency of the active mode. The sum is over all vibrational levels from $v = 0$ to u_m. u_m is the maximum vibrational quantum number that is truncated in the ground S_0 state. $1/\Gamma_{pr}$ denotes the bandwidth of the SEP laser pulse. The Franck−Condon factor is denoted by $\langle s_0 u | s_1 v \rangle$, the overlap integral of the vibrational wave functions, which is expressed[42] in terms of the displaced harmonic oscillator basis:

$$\langle s_0 u | s_1 v \rangle = (v!u!)^{1/2} \exp(-S/2) \sum_{i=0}^{v} \sum_{j=0}^{u} \frac{(-1)^j \delta_{u-j,v-i} S^{(i+j)/2}}{i!j!(v-i)!} \quad (4)$$

where $S = \omega d^2/(2\hbar)$ is the coupling constant. Huang−Rhys factor S depends strongly on d, the displacement of the equilibrium positions of two potential surfaces.

$B_{v,v}(\omega_{pr}, \tau)$ is time-dependent, describing the solvation dynamics of the excited state. Prior to the absorption of a photon, the solvent molecules are in equilibrium with the

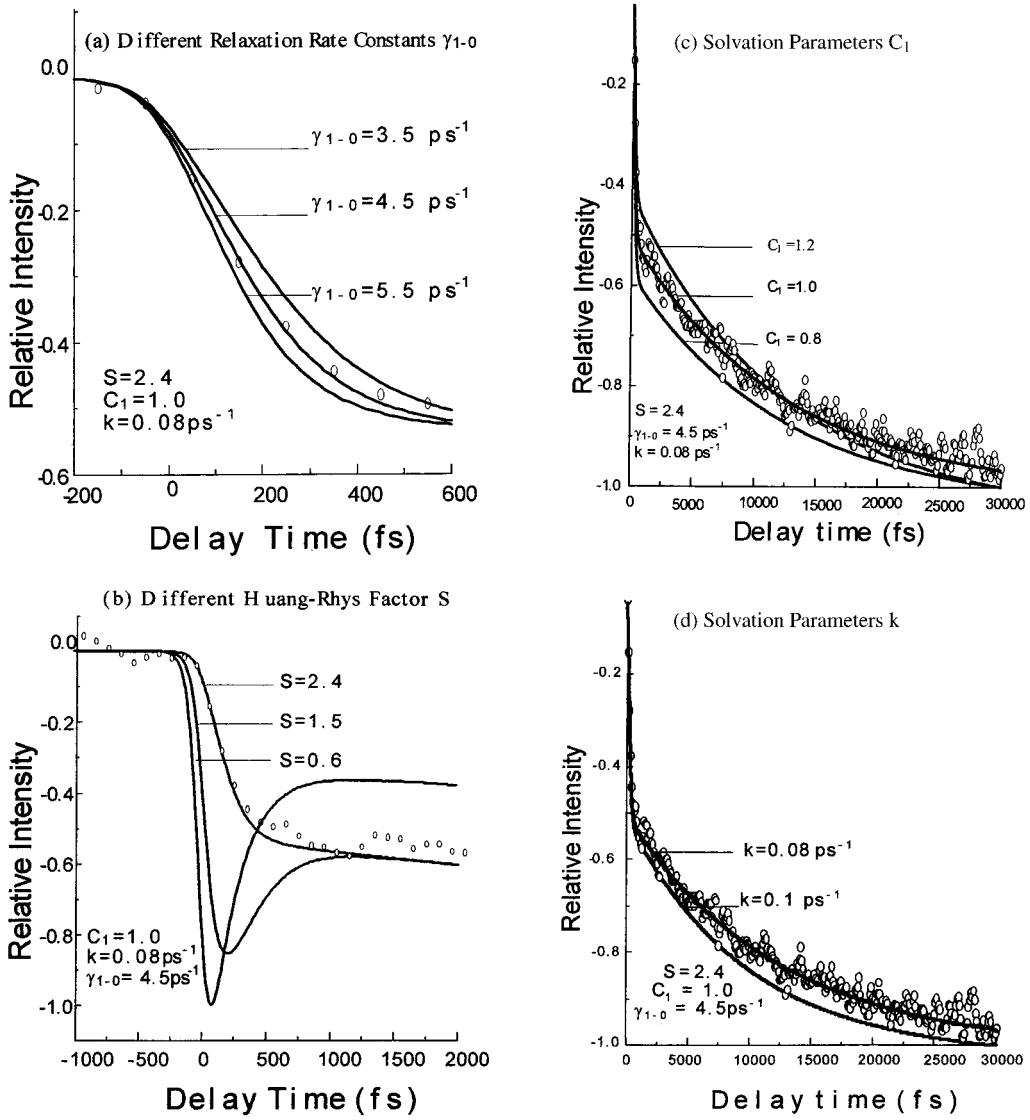

Figure 5. Simulated curves with different parameters compared with the experimental data (○).

ground-state solute molecule. Upon excitation, the solute−solvent system undergoes a Franck−Condon transition to the S_1 state in which the solute dipole has its excited-state value, but the solvent molecules still occupy their previous configuration. Then the solvent molecules reorientate to a configuration of lower energy in equilibrium with the excited solute molecule. In this process, the change of the dipole moment and the potential energy surface would change the stimulated emission effect of the solute molecule. Thus, C_1 and k are two parameters relating to the excited solvation.

By application of the ladder model,[48] in which the rate constant of vibrational transition $v \rightarrow v - 1$ is proportional to the quantum number of v, the vibrational population $\rho_{v,v}(\tau)$ satisfies the equation[42]

$$\frac{\partial \rho_{v,v}(\tau)}{\partial t} = (1+v)\gamma_{1\rightarrow 0}\rho_{v+1,v+1}(\tau) - v\gamma_{1\rightarrow 0}\rho_{v,v}(\tau) - (1+v)\times \exp\left(\frac{-\hbar\omega}{k_B T}\right)\gamma_{1\rightarrow 0}\rho_{v,v}(\tau) + v\exp\left(\frac{-\hbar\omega}{k_B T}\right)\gamma_{1\rightarrow 0}\rho_{v-1,v-1}(\tau) \quad (5)$$

The first term of eq 5 represents the population increment from $v + 1$. The second term denotes the depopulation to the $v - 1$ level. The third and the last term are the changes due to the thermal activation. The $\gamma_{1\rightarrow 0}$ represents the vibrational relaxation rate constant of the transition $v = 1 \rightarrow v = 0$. k_B is the Boltzmann constant.

The fluorescence depletion signal $S(\omega_{pr}, \tau)$ measures the response to the SEP intersity $I(\omega_{pr}, \tau)$ at a given frequency, where the time resolution is determined by the instrument response function $C(t)$ with the $\text{sech}^2\, t$ type, which is given by

$$S(\omega_{pr}, \tau) = \int_{-\infty}^{\infty} C(t) I(\omega_{pr}, \tau - t)\, dt \quad (6)$$

IV. Result and Discussion

The SEP signal $S(\omega_{pr}, \tau)$ depends on the parameters S, $\gamma_{1\rightarrow 0}$, C_1, and k. By the careful selection of suitable parameters, the observed SEP curves can be simulated. Only the C−C skeleton modes with frequency $\omega = 1500\ \text{cm}^{-1}$ of the dye molecule LDS698 is considered for the transition of the S_0 state to the S_1 state. A single vibrational mode is assumed. The vibrational transition rate constant $\gamma_{1\rightarrow 0}$ and the Huang−Rhys factor S are set to be 4.5 ps^{-1} and 2.4, respectively. Starting from the populations of $\rho_{v,v}(0) = 1$ with $v = v_m$ and $\rho_{v,v}(0) = 0$ with $v \neq v_m$, the population $\rho_{v,v}(\tau)$ of the vibrational states $v = 0-4$ at different time τ is calculated with eq 5. The time evolution of the population for $v = 0-4$ is clearly seen in Figure 4. The vibrational relaxation is due to the intramolecular vibrational energy redistribution (IVR). For dye molecules, vibrational states are very dense (10^2-10^8 per cm^{-1})[3]. The anharmonic coupling among different vibrational modes allows energy flow from the initially excited mode to other modes. It is seen in Figure 4 that the relaxation has been almost completed in 1.0 ps.

Three simulated curves with different relaxation rate constants $\gamma_{1\rightarrow 0} = 3.5$, 4.5, and 5.5 ps^{-1} are shown in Figure 5a. Only the case of $\gamma_{1\rightarrow 0} = 4.5\ \text{ps}^{-1}$ fits the observed SEP curve. In Figure 5b, three curves show the Huang−Rhys factor $S = 2.4$, 1.5, and 0.6. It can be seen that the SEP intensity strongly depends on the S value, while 2.4 is the best value. The parameter C_1 reflects the relative contribution of the excited solvation effect in the SEP signal. Three calculated curves with the parameter $C_1 = 1.40$, 1.0, and 0.8 are shown in Figure 5c,

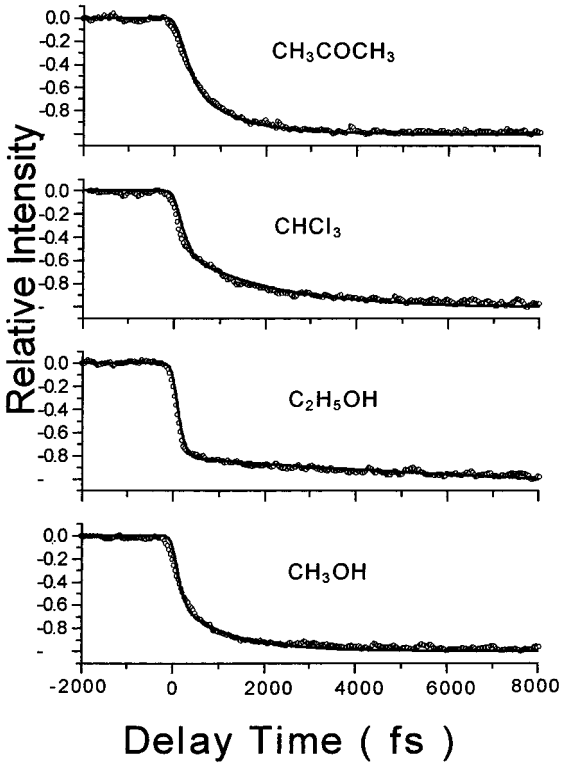

Figure 6. Time-resolved fluorescence depletion of dye LDS765 in different solvents. The open circles represent experimental data, and the lines represent the simulated results.

TABLE 1: Vibrational Relaxation Rate Constants and Parameters Relating to the Excited-State Solvation of LDS698, LDS751, and LDS765

dye	solvent	S	$\gamma_{1\rightarrow 0}$ (ps^{-1})	C_1	k (ps^{-1})
LDS698	PC:EG	2.4	4.5	1.0	0.08
LDS751	PC:EG	1.3	6.5	0.7	0.07
LDS765	PC:EG	0.6	2.3	0.6	0.07

and $C_1 = 1.0$ is the best-fitted one. Finally, k is the excited solvation rate parameter. This parameter depends strongly on the solvent used. Solvation encompasses a wide range of different intermolecular interactions. Dispersion, induced-dipole interactions, dipole−dipole or higher-order multipolar interactions, and specific interactions such as hydrogen bonding may all contribute to solvation in a given system. The simulation results with different parameters k are shown in Figure 5d. Obviously, the simulated curve of $k = 0.08\ \text{ps}^{-1}$ fits the experimental results well.

Table 1 shows the values of Huang−Rhys factor S, the vibrational relaxation rate constant $\gamma_{1\rightarrow 0}$, the parameters C_1, and the solvation rate constant k. The S and $\gamma_{1\rightarrow 0}$ values of the three molecules are different, but their k values are similar. The molecular ultrafast process is affected by different solvents. Figure 6 shows the SEP FD signals of LDS765 dissolved in acetone, chloroform, ethanol, and methanol. The simulated curves are also shown in Figure 6. The best-fitted values of S, $\gamma_{1\rightarrow 0}$, C_1, and k are shown in Table 2. The vibrational relaxation rate constants $\gamma_{1\rightarrow 0}$ of a few ps^{-1} are consistent with previous results.[49,50] $\gamma_{1\rightarrow 0}$ is also affectd by solvents in our results.

The Huang−Rhys factor S reflects the displacement of the S_0 and S_1 potential curves. A large S value correspends to a wide band-broadening in the absorption spectrum and a big Stokes shift between the absorption and the fluorescence spectra. The trend from LDS698 ($S = 2.4$) and LDS751 ($S = 1.3$) to

TABLE 2: Vibrational Relaxation Rate Constants and Parameters Relating to the Excited-State Solvation of LDS765 in Different Solvents

dye	solvent	S	$\gamma_{1\to0}$ (ps^{-1})	C_1	k (ps^{-1})	viscosity of solvent
LDS765	acetone	0.6	3.5	1.2	1.0	0.306
LDS765	chloroform	0.6	4.5	1.0	0.5	0.537
LDS765	ethanol	0.6	6.5	0.6	0.06	1.074
LDS765	methaol	0.6	6.5	0.8	0.9	0.544

LDS765 ($S = 0.6$) is consistent with the observed Stokes shift, which is about 5900, 4400,and 3300 cm^{-1} respectively. However, although the S factor of LDS765 has a small value of 0.6, its absorption band is even broader than that of the other two molecules. Also, a shoulder at 490 nm appears in the absorption spectrum. The facts implicate that a multimode coupling of the electronic transition may occur in the LDS765 molecule, as in the cases of oxazine-1[44] and photosynthetic reaction centers.[51]

It seems that the relaxation rate is influenced by the hydrogen bond between the solute and the solvent molecules. The $\gamma_{1\to0}$ value of 6.5 ps^{-1} for methanol and ethanol is larger than 4.5 ps^{-1} for chloroform and 3.5 ps^{-1} for acetone. The hydrogen atom of the −OH group can bond to an N, O, or S atom of the chromophore of the dye molecule. Such binding promises a strong solvent-assisted IVR effect.

The solvent causes a direct, and therefore more serious, effect on the excited solvation rate constant k. Since the solvation process includes reorientation of the solvent molecules, it is inferred that the solvation rate depends on the viscosity of the solvent. From Table 2, it is found that the larger the viscosity of the solvent, the smaller the k value.

Acknowledgment. We thank Professor S. H. Lin for giving us his encouragement. This work was supported by the Project of China Postdoctoral Science Foundation and the National Natural Science Foundation of China.

References and Notes

(1) Stratt, R. M.; Maroncelli, M. *J. Phys. Chem.* **1996**, *100*, 12981.
(2) Owrutsky, J. C.; Raftery, D.; Hochstrasser, R. M. *Annu. Rev. Phys. Chem.* **1994**, *45*, 519.
(3) Elsaesser, T.; Kaiser, W. *Annu. Rev. Phys. Chem.* **1991**, *42*, 83.
(4) Barbara, P. F.; Jarzeba, W. *Adv. Photochem.* **1990**, *15*, 1.
(5) Miller, D. W.; Adelman, S. A. *Int. Rev. Phys. Chem.* **1994**, *13*, 359.
(6) Ravichandran, S.; Bagchi, B. *Int. Rev. Phys. Chem.* **1995**, *14*, 271.
(7) Nitzan, A.; Mukamel, S.; Jortner, J. *J. Chem. Phys.* **1975**, *63*, 200.
(8) Seshadri, V.; Kenkre, V. M. *Phys. Rev. A* **1978**, *17*, 223.
(9) Oxtoby, D. W. *Adv. Chem. Phys.* **1981**, *47*, 487.
(10) Valle, R. G. D.; Fracassi, P. F.; Righini, R.; Califano, S. *Chem. Phys.* **1983**, *74*, 179.
(11) Adelman, S. A.; Muralidhar, R.; Stote, R. H. *J. Chem. Phys.* **1991**, *95*, 2738.
(12) Kenkre, V. M.; Tokmakoff, A.; Fayer, M. D. *J. Chem. Phys.* **1994**, *101*, 10618.
(13) Biswas, R.; Bagchi, B. *J. Phys. Chem.* **1996**, *100*, 1238.
(14) Chandra, A.; Wei, D.; Patey, G. N. *J. Chem. Phys.* **1993**, *99*, 4926.
(15) Friedman, H. L.; Raineri, F. O.; Hirata, F.; Perng, B. C. *J. Stat. Phys.* **1995**, *78*, 239.
(16) Olender, R.; Nitzan, A. *J. Chem. Phys.* **1995**,*102*, 7180.
(17) Bursulaya, B.; Zichi, D. A.; Kim, H. J. *J. Phys. Chem.* **1995**, *99*, 10069.
(18) Brown, R. *J. Chem. Phys.* **1995**, *102*, 9059.
(19) Muino, P. L.; Callis, P. R. *J. Chem. Phys.* **1994**, *100*, 4093.
(20) Benjamin, I. *Chem. Phys.* **1994**, *180*, 287.
(21) Mitsunaga, M.; Tang, C. L. *Phys. Rev. A* **1987**, *35*, 1720.
(22) Metiu, H.; Engel, V. *J. Chem. Phys.* **1990**, *93*, 5693.
(23) Fried, L. E.; Mukamel, S. *Adv. Chem. Phys.* **1993**, *84*, 435.
(24) Lin, S. H.; Fain, B.; Hamer, N. *Adv. Chem. Phys.* **1990**, *79*, 133.
(25) Pollard, W. T.; Mathies, R. A. *Annu. Rev. Phys. Chem.* **1992**, *43*, 497.
(26) Baumert, T.; Engel, V.; Meier, C.; Gerber, G. *Chem. Phys. Lett.* **1992**, *200*, 6410.
(27) Sugawara, M.; Fujimura, Y. *Chem. Phys.* **1993**, *175*, 323.
(28) Ebel, G.; Schinke, R. *J. Phys. Chem.* **1994**, *101*, 1865.
(29) Banin, U.; Bartana, A.; Ruhman, S.; Kosloff, R. *J. Chem. Phys.* **1994**, *101*, 8461.
(30) Seidner, L.; Stock, G.; Domcke, W. *Chem. Phys. Lett.* **1994**, *228*, 665.
(31) Ashworth, S. H.; Hasche, T.; Woerner, M.; Riedle, E.; Elsaesser, T. *J. Chem. Phys.* **1996**, *104*, 5761.
(32) Laermer, F.; Israel, W.; Elsaesser, T. *J. Opt. Soc. Am. B* **1990**, *7*, 1604.
(33) Weiner, A. M.; Ippen, E. P. *Chem. Phys. Lett.* **1985**, *114*, 456.
(34) Taylor, A. J.; Erskine D. J.; Tang, C. L. *Chem. Phys. Lett.* **1984**, *103*, 430.
(35) Mokhtari, A.; Chesnoy, J.; Laubereau, A. *Chem. Phys. Lett.* **1989**, *155*, 593.
(36) Mokhtari, A.; Chebira, A.; Chesnoy, J. *J. Opt. Soc. Am. B* **1990**, *7*, 1551.
(37) Horng, M. L.; Gardecki, J. A.; Papazyan, A.; Maroncelli, M. *J. Phys. Chem.* **1995**, *99*, 17311.
(38) Blanchard, G. J. *J. Chem. Phys.* **1991**, *95*, 6317.
(39) Cho, M.; Rosenthal, S. J.; Scherer, N. F.; Ziegler, L. D.; Fleming, G. R. *J. Chem. Phys.* **1992**, *96*, 5033.
(40) Bingemann, D.; Ernsting, N. P. *J. Chem. Phys.* **1995**, *102*, 2691.
(41) Zhong, Q. H.; Wang, Z. H.; Sun, Y.; Zhu, Q. H.; Kong, F. A. *Chem. Phys. Lett.* **1996**, *248*, 277.
(42) Gu, X. Z.; Hayashi, M.; Suzuki, S.; Lin, S. H. *Biochim. Biophys. Acta* **1995**, *1229*, 215.
(43) Colthup, N. B.; Daly, L. H.; Wiberley, S. E. *Introduction to Infrared and Raman Spectroscopy*; Academic Press: New York, 1964; p 224.
(44) Scherer, P. O. J.; Seilmeier, A.; Kaiser, W. *J. Chem. Phys.* **1985**, *83*, 3948.
(45) Lin, S. H.; Alden, R. G.; Tang, C. K.; Fujimura, Y.; Sugawara, M. *Mode Selective Chemistry*; Jortner, J., et al., Eds.; Kluwer: Dordrecht, 1991; p 467.
(46) Fain, B.; Lin, S. H.; Hamer, N. *J. Chem. Phys.* **1989**, *91*, 4485.
(47) Lin, S. H.; Alden, R. G.; Islampour, R.; Ma, H.; Villaeys, A. A. *Density Matrix Method and Femtosecond Processes*; World Scientific: Singapore, 1991.
(48) Lin, S. H. *J. Chem. Phys.* **1974**, *61*, 3810.
(49) Herrmann, J.; Wilhelmi, B. *Laser for Ultrashort Light Pulses*; North-Holland: Amsterdam, 1987; p 34.
(50) Zewail, A. H. *J. Phys. Chem.* **1996**, *100*, 12701.
(51) Lin, S. H.; Hayashi, M.; Suzuki, S.; Gu, X.; Xiao, W.; Sugawara, M. *Chem. Phys.* **1995**, *197*, 435.